

The stabilizing role of differential rotation on hydromagnetic waves

By D. R. FEARN AND M. R. E. PROCTOR

Department of Applied Mathematics and Theoretical Physics,
Silver Street, Cambridge CB3 9EW

(Received 17 June 1982 and in revised form 9 November 1982)

The role that differential rotation plays in the hydromagnetic stability of rapidly rotating fluids has recently been investigated by Fearn & Proctor (1983) (hereinafter referred to as I) as part of a wider study related to the geodynamo problem. Starting with a uniformly rotating fluid sphere, the strength of the differential rotation was gradually increased from zero and several interesting features were observed. These included the development of a critical region whose size decreased as the strength of the shear increased. The resolution of the two-dimensional numerical scheme used in I is limited, and consequently it was only possible to consider small shear strengths. This is unfortunate because differential rotation is probably an important effect in the Earth's core and a more detailed study at higher shear strengths is desirable. Here we are able to achieve this by studying a rapidly rotating Bénard layer with imposed magnetic field $\mathbf{B}_0 = B_M s \hat{\phi}$ and shear $\mathbf{U}_0 = U_M s \Omega(z) \hat{\phi}$, where (s, ϕ, z) are cylindrical polar coordinates. In the limit where the ratio q of the thermal to magnetic diffusivities vanishes ($q = 0$), the governing equations are separable in two space dimensions and the problem reduces to a one-dimensional boundary-value problem. This can be solved numerically with greater accuracy than was possible in the spherical geometry of I. The strength of the shear is measured by a modified Reynolds number $R_t = U_M d / \kappa$, where d is the depth of the layer and κ is the thermal diffusivity, and the shear becomes important when $R_t \geq O(1)$. It is possible to compute solutions well into the asymptotic regime $R_t \gg 1$, and details of the behaviour observed are dependent on the nature of $\Omega(z)$. Specifically, two cases were considered: (a) $\Omega(z)$ has no turning point in $0 < z < 1$, and (b) $\Omega(z)$ has a turning point at $z = z_T$, $0 < z_T < 1$ ($\Omega'(z_T) = 0$, $\Omega''(z_T) \neq 0$). In both cases, as R_t increases a critical layer centred at $z = z_L$ develops, with width proportional to (a) $R_t^{-\frac{1}{2}}$, (b) $R_t^{-\frac{1}{4}}$. In the case where $\Omega(z)$ has a turning point, the critical layer is located at the turning point ($z_L = z_T$). The critical Rayleigh number R_c increases with (a) $R_c \propto R_t$, (b) $R_c \propto R_t^{\frac{3}{2}}$, and the instability is carried around with the fluid velocity at the critical layer. The relevance of these results to the geomagnetic secular variation is discussed.

1. Introduction

Fearn & Proctor (1983) (hereinafter referred to as I) have discussed the reasons for expecting differential rotation in the Earth's core and why it is likely to be of importance. They went some way in investigating how shear in the basic rotation modifies various modes of hydromagnetic waves and instabilities, but the study was limited by the lack of numerical resolution in the spherical geometry considered there. In other studies of the onset of convection in rapidly rotating systems the role of differential rotation has been badly neglected (see reviews by Roberts & Soward 1972;

Acheson & Hide 1973; Acheson 1978; Roberts 1978; Eltayeb 1981). This has not been because of a lack of recognition of its importance but rather because of the mathematical difficulties it adds to an already complex problem. The effect of differential rotation has received some attention recently, though, and a little progress has been made toward an understanding of its role.

In a diffusionless model with a cylindrical geometry, Acheson (1973) studied the stability of the basic state with magnetic field $\mathbf{B}_0 = B_0(s)\hat{\phi}$ and flow (with respect to a rapid uniform rotation) $\mathbf{U}_0 = U_0(s)\hat{\phi}$. Most of Acheson's results are for $\mathbf{U}_0 = 0$ and he is only able to speculate on the effect on his stability criteria of adding a non-zero flow. The inclusion of a non-zero \mathbf{U}_0 proves too much for the global analysis, but in a later paper Acheson (1982) has used a local analysis to investigate the stability of the basic state

$$\mathbf{B}_0 = B_0(s)\hat{\phi}, \quad \mathbf{U}_0 = U_0(s)\hat{\phi}, \quad (1.1)$$

in a model that incorporates buoyancy as well as diffusion. The global analysis of Acheson (1973) (see also Acheson 1972) had shown a positive outward gradient of B_0/s to be destabilizing. The local analysis supports this and also shows that a positive outward gradient of U_0/s is stabilizing. These results apply both to the diffusionless magnetic-field-gradient instability (Acheson 1972, 1973, 1978) and the buoyancy-catalysed instability (Roberts & Loper 1979; Soward 1979; Fearn 1979; Acheson 1980) which derive their energy from the basic magnetic field (or from the basic flow), but have very different instability mechanisms and operate on different timescales. An extension of the local analysis to cover the basic state

$$\mathbf{B}_0 = B_0(s, z)\hat{\phi}, \quad \mathbf{U}_0 = U_0(s, z)\hat{\phi} \quad (1.2)$$

has been made in I. The presence of z -structure in the basic state was found to be destabilizing, and this conclusion was supported by their global solutions. The main role of shear in this case is to permit a wider range of instability, but the results tell us nothing about how differential rotation modifies instabilities of other types which may already exist, for example thermally driven instabilities.

Braginsky (1980) has investigated how the addition of a differential rotation modifies his MAC waves (see Braginsky 1967). His model consists of a rectangular channel (the narrow-gap limit of a cylindrical annulus) with a uniform magnetic field B_0 and a sheared flow $R_t U_0(s)$ directed down the channel. He considers three cases: (a) the basic model with no diffusion and no buoyancy; (b) as (a) but with ohmic diffusion; and (c) as (a) but with buoyancy. In all three cases he finds an increasing shear-flow strength R_t to be accompanied by a shortening of the lengthscale in the direction of $\nabla(U_0/s)$ (the \hat{s} -direction), with the lengthscale inversely proportional to R_t . The shortening lengthscale means that diffusion must become important, as Braginsky (1980) recognized but he was unable simultaneously to incorporate both diffusion and the buoyancy force required to maintain the instability against ohmic losses. Adding only the effect of ohmic diffusion he finds a tendency for the eigenfunctions to be peaked. This happens where the lengthscale is longer and the dissipation less. Braginsky then neglects the diffusion and incorporates a buoyancy force. The criterion for the instability of MAC waves (in the diffusionless model) is independent of the differential-rotation strength, but increasing R_t still results in the shortening of the s -lengthscale. The solution is also observed to become localized around some radius s_L with the width of the localized region $O(R_t^{-1/2})$.

Braginsky's (1980) work has demonstrated some of the important effects due to differential rotation, but it is clear that many aspects of the problem remain to be investigated. The observed shortening of lengthscale means that it is essential to

incorporate dissipation into the model. This will have the effect of damping the (diffusionless) MAC wave instability so some forcing must also be included. The presence of diffusion increases the order of the system of equations describing the problem, and new, diffusive, modes of instability are introduced. The effect of the differential rotation on these must also be investigated, especially since these modes are preferred over the MAC wave mode when the magnetic diffusivity exceeds the thermal diffusivity (see Fearn 1979), as is thought to be the case in the core. A further area that requires attention is the limit $R_t \gg 1$. Except in very idealized cases, the problem requires a numerical solution, and the shortening of lengthscale with increasing R_t means that the greater the shear the greater the numerical resolution required. Braginsky (1980), with limited computing facilities, was unable to consider very large shear strengths.

Our first approach to tackling some of these points is described in I, where an attempt was made to construct (and solve) a model of the core which is much more realistic than those of previous authors. Any basic state of the form (1.2) could be considered, the geometry was spherical, and both diffusion and thermal buoyancy were included. The generality of the model had of course to be paid for; the problem required a two-dimensional numerical solution and resolution was limited. Nevertheless it was possible to investigate the role of differential rotation on the diffusive modes of instability and an interesting behaviour was observed. As the strength of the differential rotation was increased, the perturbation in the temperature became increasingly localized. At first sight this appeared to be the same phenomenon as observed by Braginsky (1980), but, as we shall show later, it is quite different. The peaking of the temperature perturbation is due to the development of a critical layer. Outside the layer thermal diffusion is unimportant, but in the layer the phase speed of the wave approaches the speed of the fluid and thermal diffusion is required in the leading-order balance. However, there is no shortening of lengthscale except in the critical layer, in contrast with Braginsky's diffusionless theory. As already mentioned, the numerical method of I is incapable of resolving the critical layer for $R_t \gg 1$, so a simpler model is required to investigate in detail the role of differential rotation. The two essential requirements of such a model are that it retain the physics of the spherical problem but that its solution can at least be reduced to a numerical solution of an ordinary differential equation.

Our understanding of several types of instability was greatly improved by a simple model due to Soward (1979) (hereinafter referred to as S79), who considered a rapidly rotating Bénard layer with applied magnetic field $\mathbf{B}_0 = B_M s \hat{\phi}$. The resulting linear stability equations are separable in all three space dimensions and the problem reduces to the solution of a system of algebraic equations, permitting a detailed study of the many modes of instability present. This approach seems promising so we shall take Soward's model as our starting point and introduce a sheared flow $\mathbf{U}_0 = U_M s \Omega(z) \hat{\phi}$ to investigate the role of differential rotation. It should be emphasized that the basic state is now rather artificial since we have provided no mechanism for generating \mathbf{U}_0 , and it cannot be specified arbitrarily if $B_0 \neq 0$. Nevertheless (as discussed in I) there are so many causes of shear in a convecting, rapidly rotating, hydromagnetic system that we feel useful information can be gained from a study where \mathbf{U}_0 is chosen and varied independently. Retention of separation of variables in all three directions is now of course impossible, but provided we restrict ourselves to the diffusive modes investigated in I (which operate on the thermal diffusion timescale) and take the limit $q = 0$ (where $q = \kappa/\eta$ is the ratio of the thermal to magnetic diffusivities) the problem is separable in s and ϕ as well as time t (see §2 for details). The resulting

system of ordinary differential equations in z then has to be solved numerically, but the resolution available enables asymptotically large values of the shear to be considered. The numerical results are given in §3, they are discussed in §4, and concluding remarks are made in §5.

2. The model, simplifications and method of solution

In this section we first describe in detail the model under consideration and the equations governing its linear stability. Various simplifications are made, limiting the scope of the model by filtering out certain modes of instability but retaining those in which we are interested and ensuring the equations are separable in two space dimensions. The system of equations is essentially the same as that in I (I2.3). The main differences are the geometry, the basic state, and the boundary conditions. Here we shall be considering an electrically conducting fluid confined between two infinite parallel flat plates separated by a distance d . There is a temperature difference ΔT between the lower and upper plates, and the whole system is rapidly rotating with angular velocity $\boldsymbol{\Omega}_0 = \Omega_0 \hat{\mathbf{z}}$ about an axis normal to the layer. The fluid is permeated by a magnetic field \mathbf{B}_0 , and is moving relative to the rotating frame with velocity \mathbf{U}_0 given by

$$\mathbf{B}_0 = B_M s \hat{\boldsymbol{\phi}}, \quad \mathbf{U}_0 = U_M s \Omega(z) \hat{\boldsymbol{\phi}}. \quad (2.1)$$

To keep the boundary conditions simple we shall take the upper and lower plates to be perfect electrical and thermal conductors. The non-dimensional parameters are as defined in (I2.5) if we replace r_0 by d and set $\beta = \Delta T/d$. Since this study is restricted to thermal diffusion timescale instabilities, it is convenient to have the non-dimensionalization on this timescale (rather than the magnetic diffusion timescale used in I). This requires the definition of a new dimensionless quantity

$$R_t = U_M d / \kappa, \quad (2.2)$$

and also results in $\mathbf{b} \rightarrow q\mathbf{b}$, $\mathbf{u} \rightarrow q\mathbf{u}$ and $t \rightarrow q^{-1}t$ in (I2.3).

As in I, we are interested in the parameter range $\Lambda = O(1)$ so viscous and inertial terms will again be neglected. Neglecting viscosity means that we must impose only one boundary condition on the fluid velocity; that of no normal flow at $z = 0, 1$. Neglecting inertia has the effect of filtering out inertial timescale instabilities. As it stands (I2.3) is separable in ϕ and t , but the presence of the term $qR_t \nabla \times (\mathbf{U}_0 \times \mathbf{b})$ in the induction equation (I2.3*b*) prevents separation in s . The diffusive instabilities studied in I operate on the thermal diffusion timescale and we are interested in small values of q (the molecular diffusivity ratio in the Earth's core is $q \sim 10^{-6}$), so to make our problem more tractable we shall take the formal limit $q = 0$. This has the effect of removing the offending term in the induction equation, but at the same time limits us to investigating only instabilities on the thermal diffusion timescale. These include the thermally driven diffusive instability and the magnetically driven buoyancy-catalysed instability of I.

The continuity equations (I2.3*d, e*) are automatically satisfied by expanding \mathbf{u} and \mathbf{b} into poloidal and toroidal parts:

$$k^2 \mathbf{u} = \nabla \times \omega \hat{\mathbf{z}} + \nabla \times \nabla \times w \hat{\mathbf{z}}, \quad k^2 \mathbf{b} = \nabla \times j \hat{\mathbf{z}} + \nabla \times \nabla \times b \hat{\mathbf{z}}, \quad (2.3)$$

where ω , w , j and b are the vertical ($\hat{\mathbf{z}}$) components of the vorticity, velocity, current and magnetic field respectively, and k is the radial wavenumber defined below. The

governing equations with $q = 0$ are separable in s , ϕ and t , so we expand all variables in the form

$$v(s, \phi, z, t) = v(z) J_m(ks) e^{im\phi} e^{pt}, \quad (2.4)$$

where v stands for any of the variables p , ω , w , j , b or ϑ . Substituting (2.3), (2.4) into (I2.3) and taking $\mathbf{z} \cdot \nabla \times$ (I2.3a), $\mathbf{z} \cdot \nabla \times \nabla \times$ (I2.3a), $\mathbf{z} \cdot$ (I2.3b), $\mathbf{z} \cdot \nabla \times$ (I2.3b) and (I2.3c) we obtain

$$-Dw = \Lambda(-2Db + imj), \quad (2.5a)$$

$$-D\omega = \Lambda(-2Dj + im(k^2 - D^2)b) + k^2 R\vartheta, \quad (2.5b)$$

$$0 = imw + (D^2 - k^2)b, \quad (2.5c)$$

$$0 = im\omega + (D^2 - k^2)j, \quad (2.5d)$$

$$w = (p + imR_t \Omega(z) + k^2 - D^2)\vartheta, \quad (2.5e)$$

where D denotes the differential operator d/dz . Our problem has reduced to an eighth-order system of ordinary differential equations subject to the boundary conditions

$$w = \vartheta = b = Dj = 0 \quad (z = 0, 1). \quad (2.6)$$

This system requires a numerical solution, and some elimination of variables is helpful. Using (2.8 c, d) to eliminate w and ω , (2.8 a, b, e) become

$$\begin{aligned} (D^2 - k^2 + 2im\Lambda) Db + \Lambda m^2 j &= 0, \\ (D^2 - k^2 + 2im\Lambda) Dj - \Lambda m^2 (D^2 - k^2) b - imk^2 R\vartheta &= 0, \\ (D^2 - k^2 - imR_t \Omega(z)) \vartheta + (i/m)(D^2 - k^2) b &= p\vartheta, \end{aligned} \quad (2.7)$$

and this is the system we shall solve numerically. It is instructive though to reduce (2.10) further to a single equation

$$\begin{aligned} \{[(D^2 - k^2) - i(mR_t \Omega(z) - \omega)] [(D^2 - k^2 + 2im\Lambda)^2 D^2 + \Lambda^2 m^4 (D^2 - k^2)] \\ + R\Lambda m^2 k^2 (D^2 - k^2)\} b = 0, \end{aligned} \quad (2.8)$$

where $\omega = ip$ is the frequency of the instability. We can see from (2.8) that when $R_t \gg 1$ a critical layer will develop where the phase speed of the wave matches the fluid velocity ($\omega = mR_t \Omega(z)$), and this determines the form of the numerical solution. Some details of the numerical methods used are given in appendix A.

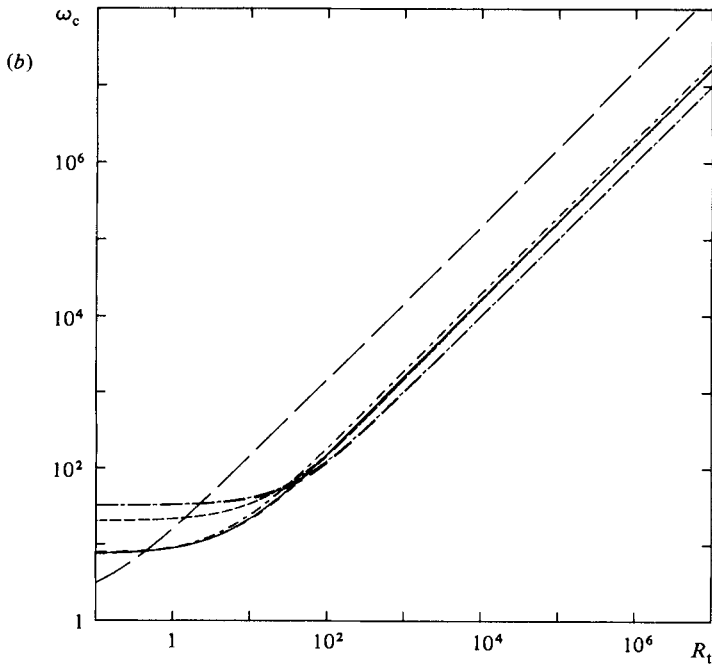
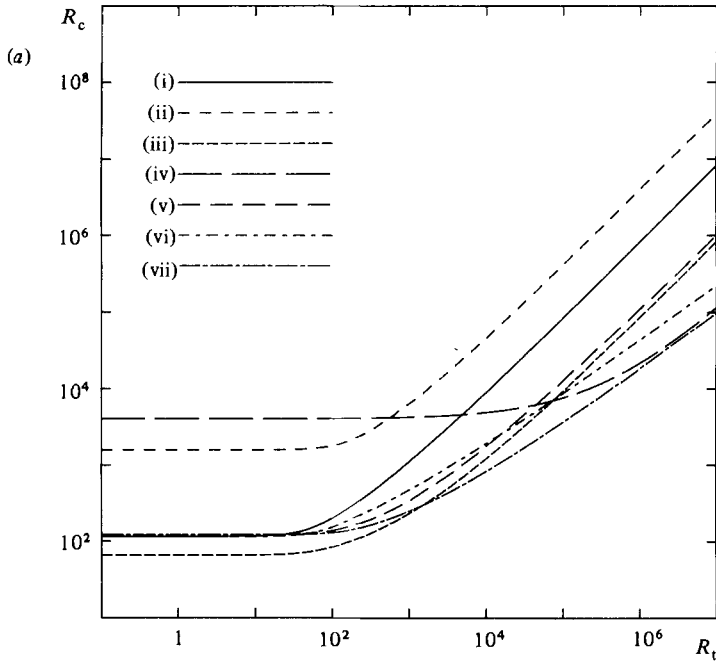
3. Numerical results

The analysis of §2 was completed while leaving the differential rotation $\Omega(z)$ unspecified, but before a numerical solution can be computed it is necessary to prescribe $\Omega(z)$. As long as $\Omega(z)$ is not constant, a critical layer must be present (see (2.8)) so we expect that the precise choice of $\Omega(z)$ will not be important. However, since the nature of the critical layer is determined by a balance between the term $D^2 b$ and $i(mR_t \Omega(z) - \omega) b$ in (2.8) it is necessary to distinguish between flows that have a turning point in the layer ($\Omega'(z_T) = 0$, $0 < z_T < 1$) and those that do not. For this purpose we have chosen to study two flows. The first,

$$\Omega_1(z) = 1 - z^2, \quad (3.1)$$

has no turning point within the layer and is the flow used for most of the results to be presented. The second,

$$\Omega_2(z) = 4z(1 - z), \quad (3.2)$$



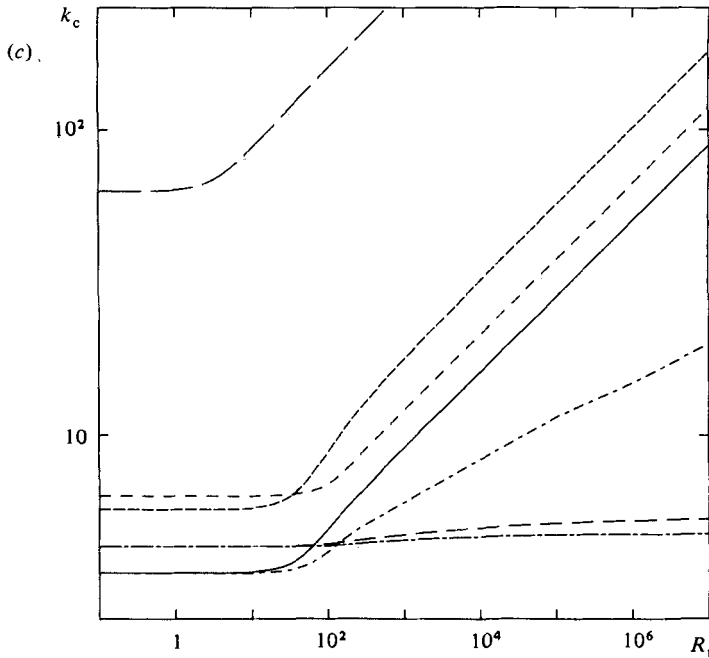


FIGURE 1. The effect of adding a differential rotation is illustrated with graphs of (a) R_c , (b) ω_c and (c) k_c against R_t . The cases shown are: for $\Omega = 1 - z^2$ (i) $\Lambda = 1, m = 2, n = 1$; (ii) $\Lambda = 1, m = 2, n = 2$; (iii) $\Lambda = 10, m = 2, n = 1$; (iv) $\Lambda = 10, m = 20, n = 1$; (v) $\Lambda = 100, m = 1, n = 1, R < 0$; and for $\Omega = 4z(1 - z)$ (vi) $\Lambda = 1, m = 2, n = 1$; (vii) $\Lambda = 100, m = 1, n = 1, R < 0$. In cases (i)–(iv) and (vi), where the frequency ω_c is initially negative ($\omega_c(R_t = 0) < 0$), a constant $-2\omega_c(R_t = 0)$ has been added to ω_c to facilitate plotting on a logarithmic scale. The code shown in (a) applies also to (b) and (c).

has a turning point at $z = \frac{1}{2}$. Some calculations were made with a third flow $\Omega_3(z) = \frac{1}{2}z(1 + z)$, but the results were qualitatively the same as those obtained using (3.1).

The problem described in §2 reduces to that of S79 in the limit $R_t = 0$. This provides a useful starting point for our numerical solutions as well as a necessary check on them. With only 50 grid points we found agreement to better than six significant figures. Several cases were investigated and the same procedure was adopted for all. With $R_t = 0$ we took the S79 solution and specified the parameters: azimuthal wavenumber m , vertical wavenumber n (the S79 solutions were separable in z and were proportional to either $\sin n\pi z$ or $\cos n\pi z$), and magnetic-field strength Λ . This done, we found the minimum critical Rayleigh number R_c by taking the frequency ω to be real (zero growth rate) and minimizing the Rayleigh number over all values of the radial wavenumber k . Taking this solution as a starting point, R_t was gradually increased and the behaviour of the chosen mode was followed until an asymptotic ($R_t \gg 1$) limit was reached. The variation of R_c , ω_c and k_c with R_t is shown in figure 1 for the various cases considered. The behaviour of the eigensolution for the case $\Lambda = 1, m = 2, n = 1$ is shown in figure 2 for a range of values of R_t and, for comparison, the asymptotic limits of the eigensolutions of the other cases at $R_t = 10^6$ are illustrated in figure 3.

In all the cases considered, it was possible to compute solutions well into the

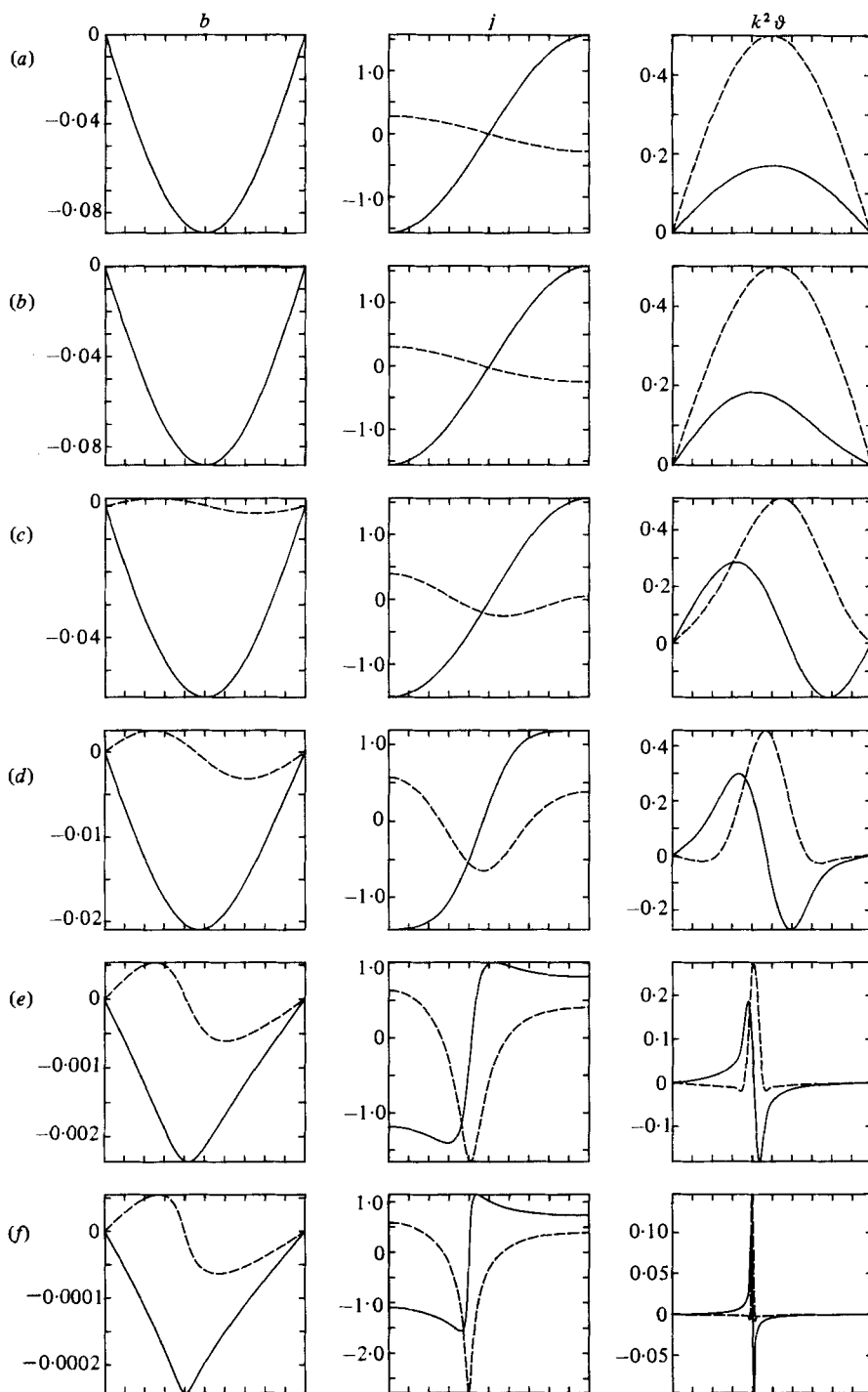


FIGURE 2. The eigensolutions for b , j and $k^2\vartheta$ when $\Lambda = 1$, $m = 2$, $n = 1$ and $\Omega = 1 - z^2$ are shown for (a) $R_t = 0$, (b) 10, (c) 10^2 , (d) 10^3 , (e) 10^5 and (f) 10^7 . The normalization of the eigenfunction has been chosen to make the maximum modulus of w equal to unity. The behaviour of w and ω are not shown as they are similar to b and j respectively (see (2.5c, d)). The horizontal scale is linear, with z taking values between 0 and 1. Both real (full line) and imaginary (dashed line) parts of the eigenfunction are shown.

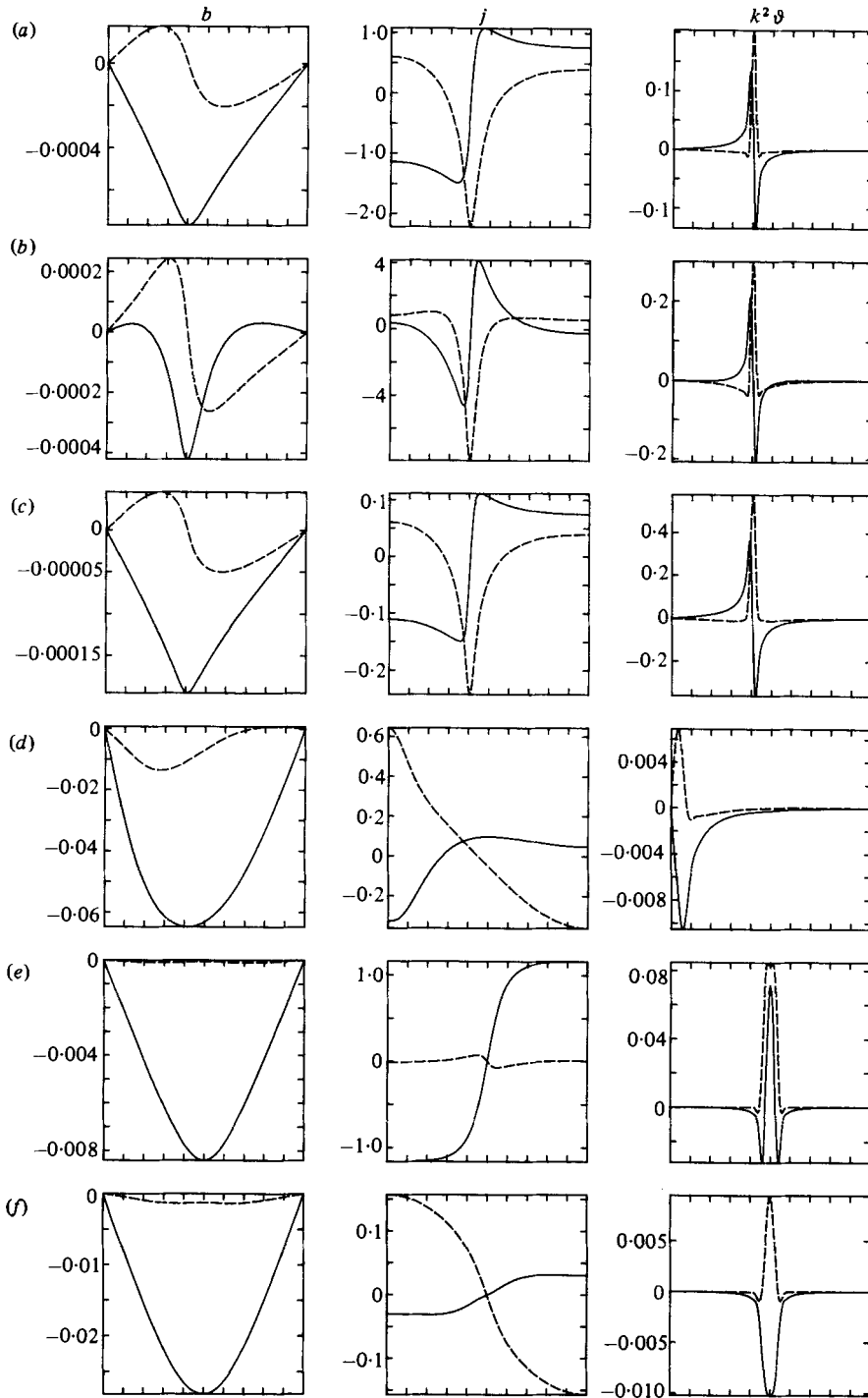


FIGURE 3. As figure 2 but for $R_t = 10^6$, $\Omega = 1 - z^2$ and (a) $\Lambda = 1$, $m = 2$, $n = 1$; (b) $\Lambda = 1$, $m = 2$, $n = 2$; (c) $\Lambda = 10$, $m = 2$, $n = 1$; (d) $\Lambda = 100$, $m = 1$, $n = 1$, $R < 0$. Cases (e) and (f) are as (a) and (d) but with $\Omega = 4z(1 - z)$.

asymptotic regime $R_t \gg 1$, and, as can be seen from figure 1, all modes with Ω given by (3.1) behave in the same manner;

$$R_c \propto R_t, \quad \omega_c \propto R_t, \quad k_c \propto R_t^{\frac{1}{2}}. \quad (3.3)$$

Similarly for differential rotation (3.2),

$$R_c \propto R_t^{\frac{3}{2}}, \quad \omega_c \propto R_t, \quad k_c \propto R_t^{\frac{1}{2}}. \quad (3.4)$$

The only exception to the above is the behaviour of the critical radial wavenumber k_c for the buoyancy-catalysed ($R < 0$) modes. Then k_c increases only very slowly with R_t , but the reason for this is evident from S79. Soward shows that for $R_t = 0$ the $R < 0$ mode can only exist for $\delta = k/n\pi < \sqrt{3}$, that is for $k < 5.44$ when $n = 1$. From the behaviour of k_c shown in figure 1(c) it appears that this condition still holds when $R_t > 0$. The contrast in the behaviour of k_c between the $R > 0$ and the $R < 0$ modes shows that, at leading order, α in the relation $k_c \propto R_t^\alpha$ is not important. This conclusion was supported by increasing R_t while keeping k fixed. The behaviour of R_c, ω_c is unchanged, though the constants of proportionality differ from those when R_c is minimized with respect to k .

When $R_t = 0$, it is the $n = 1$ solutions that are the most unstable (S79), so we have concentrated most of our attention on these modes. However, it is not possible to ignore the $n \geq 2$ modes since we cannot be certain that the $n = 1$ mode is always the most unstable when $R_t > 0$. One check is to follow an $n \geq 2$ mode to large values of R_t . The $n = 2$ mode shown in figure 1 always has a greater critical Rayleigh number than the $n = 1$ mode, and similarly the corresponding $n = 10$ mode (not illustrated) is always more stable than the $n = 2$ mode. A second check is to find all the eigenvalues of the matrix eigenvalue problem rather than just the one found by inverse iteration (see appendix A). For all the modes illustrated in figure 1 we found that the $n = 1$ mode remained the most unstable, well into the asymptotic regime at $R_t = 10^5$. The results were also consistent with the ordering of the modes being unchanged, $n = 1$ being the most unstable, $n = 2$ the next, then $n = 3$, and so on.

4. Discussion

The plane-layer model considered here has many simplifications compared with the spherical model of I, but the physics necessary to investigate the effects of differential rotation has not been lost. There are restrictions as to which classes of instability can be studied (see also §5) but the results given in §3 are consistent with those of I, and this suggests that the more detailed and extensive results of the plane-layer model should carry over to the spherical geometry. In both cases the increasing strength of differential rotation causes an increasing concentration of the instability in a critical layer. The reason for this is that there is a tendency for the instability to be carried along with the fluid flow. A perturbation to the basic state can only remain in phase on a lengthscale over which diffusion is strong enough to counteract the shear in the basic flow. The two classes of instability studied here (and in I) operate on the thermal diffusion timescale, which is taken to be much longer than the magnetic diffusion timescale. Therefore there is plenty of time for the magnetic field to diffuse and the perturbed magnetic field is not concentrated. On the other hand, thermal diffusion is much weaker and the temperature perturbation is confined to the region where thermal diffusion is strong enough to offset the tearing action of the differential rotation. The temperature perturbation is thus concentrated in a critical layer which decreases in width as the strength of the differential rotation is increased. The width of the critical layer depends also on the gradient of Ω . The steeper the gradient, the

narrower the layer. This has consequences for the location of the mode of instability that is most unstable. For a given value of R_t there is therefore a tendency for the most-unstable mode to locate itself where $d\Omega/dz$ is small. There are of course other influences, but this dominates when there is a zero in the gradient of Ω . Then, the critical layer is located where $d\Omega/dz = 0$ and the buoyancy force required for instability is smaller ($R_c \propto R_t^{\frac{3}{2}}$ compared with $R_c \propto R_t$ when there is no zero of $d\Omega/dz$). When $\Omega(z)$ has no turning point there is no simple criterion for the preferred location of the critical layer (but see appendix B). For the diffusive thermal instability an interior location is chosen in all the cases considered while the buoyancy-catalysed instability appears to prefer being located close to the boundary where Ω is largest. (This remark is based only on the common feature for flows Ω_1 and Ω_3 so should be treated with caution.) The influence of the radial wavenumber k is rather weak. It shows a tendency to increase as R_t increases, but if it is held fixed the qualitative behaviour of R_c is the same.

From the results obtained for large R_t it appears that the frequency $\omega \rightarrow mR_t \Omega(z_L)$, where z_L is the location of the critical layer. To leading order this is true, but as we shall see, at least for the case where $\Omega(z)$ has a maximum, the phase speed of the wave must have a westward component with respect to the flow in the critical layer ($\omega/m < R_t \Omega(z_L)$) when $R > 0$. This may be demonstrated by manipulating integrals of (2.5) across the layer. If we denote

$$\langle f(z) \rangle = \int_0^1 f(z) dz, \quad (4.1)$$

and a superscript $*$ denotes a complex conjugate, then take $\langle \vartheta(2.5e)^* \rangle$, $\langle w^*(2.5b) \rangle$ and $\langle Dw^*(2.5c) \rangle$. We substitute for j from (2.5a), D^2b from (2.5c), then take $\langle b(2.5c)^* \rangle$ to eliminate $\langle w^*b \rangle$. Taking the imaginary part of the resulting equation gives

$$R = \frac{4\langle |Dw|^2 \rangle}{mk^2 \langle (mR_t \Omega - \omega) |\vartheta|^2 \rangle}, \quad (4.2)$$

while the real part may be written

$$R = \frac{I(Dw) + 4\Lambda^2 k^2 I(b) + m^2 \Lambda^2 (m^2 - 4) \langle |w|^2 \rangle}{m^2 k^2 \Lambda I(\vartheta)}, \quad (4.3)$$

where

$$I(v) = \langle |Dv|^2 \rangle + k^2 \langle |v|^2 \rangle. \quad (4.4)$$

From (4.3) we can see clearly that R must be positive unless $m = 1$. (The $m = 1$, $R < 0$ mode is the buoyancy-catalysed instability discussed by Roberts & Loper (1979), Fearn (1979) and Acheson (1982).) When $R > 0$ we can see from (4.2) that $R_t \Omega(z) - \omega/m > 0$ for some z , and in the case where ϑ is sharply peaked at $z = z_L$ we must have $R_t \Omega - \omega/m > 0$ in some neighbourhood of $z = z_L$. This requirement is particularly restrictive if $\Omega(z)$ has a maximum at or close to $z = z_L$ because then $\omega/m > R_t \Omega(z)$ for all z except in the immediate neighbourhood of the critical layer.

5. Concluding remarks

The effect of differential rotation on two classes of hydromagnetic waves has been investigated using a simple model consisting of a rapidly rotating Bénard layer with an imposed azimuthal magnetic field and flow (2.1). The results obtained are qualitatively similar to those obtained in the more realistic spherical geometry (see I) but are much more detailed and extend to much greater strengths R_t of the

differential rotation. As R_t is increased above $O(1)$ values a critical layer with decreasing lengthscale develops. The two-dimensional numerical solution of I is restricted to $O(1)$ lengthscales by the available computer store and speed, but the one-dimensional boundary-value problem that has to be solved here is capable of resolving very short lengthscales and large values of R_t ($R_t \gg 1$) can be accommodated. Of course there is a price to pay for the relative simplicity of the present model. To construct a problem that is separable in the radial and azimuthal directions it is necessary to take the limit $q = 0$, which restricts the scope of the present study to instabilities operating on the thermal diffusion timescale. There are two such diffusive instabilities; one is thermally driven (the thermal diffusive instability) and the other is magnetically driven but requires some stratification to release the energy stored in the magnetic field (the buoyancy-catalysed instability). Despite their rather different characters, both classes of instability behave in a similar manner, with the stratification required for the onset of convection increasing with the strength of the differential rotation (see figure 1*a*). A critical layer develops about some location $z = z_L$ as R_t is increased and the instability is carried around with the flow at that location ($\omega = mR_t\Omega(z_L)$; see figure 1*b*). In the limit $q = 0$ the magnetic field diffuses instantaneously so there is no tendency for the field to be carried along at different speeds at different locations. (This is the opposite limit to perfect conductivity, where diffusion is negligible and the field is frozen to the fluid.) In contrast, thermal diffusion is negligible except within the critical layer. A temperature perturbation in phase with that at $z = z_L$ can only be maintained where diffusion is fast enough to counteract the effect of the shear in the basic azimuthal flow. Consequently the temperature perturbation is confined to where thermal diffusion is important; that is, in the critical layer (see figures 2 and 3).

The limit $q = 0$ is very artificial since it means that the magnetic field is unaffected by the shear in the basic flow. In practice, with q small but non-zero, we anticipate that the magnetic field will begin to feel the effect of the differential rotation when $R_t = O(q^{-1})$ (that is when the magnetic Reynolds number $R_m = U_M d/\eta = O(1)$). Then we might expect to see a concentration also of the magnetic-field perturbation, so the instability generated at z_L will be confined to the immediate vicinity of $z = z_L$. One reason for studying the diffusive thermal instability is that, when $q \lesssim 1$ and in the absence of differential rotation, it is more easily excited than the diffusionless MAC waves (Braginsky 1967) (when $\Lambda \gtrsim O(1)$, $R_c = O(\Lambda)$ for the diffusive thermal instability while $R_c = O(\Lambda/q)$ for MAC waves). However, we have seen that the differential rotation has a strong stabilizing effect on the diffusive thermal instability so the relative importance of the two classes of thermally driven instability may be dramatically changed by the presence of a strong shear. For dynamo action magnetic-field generation must exceed diffusive losses, so we must expect $R_m \gtrsim O(1)$. If $R_m = O(1)$ then $R_t = O(q^{-1})$ and, with $R_c \propto R_t$, $R_c = O(q^{-1})$ when $\Lambda = O(1)$ for the diffusive thermal instability. The MAC waves operate on the diffusionless timescale Ω_M^2/Ω , where $\Omega_M = B_M/d(\mu\rho_0)^{1/2}$ is the Alfvén angular velocity, but when $\Lambda = O(1)$ this is comparable to the magnetic diffusion timescale. We therefore expect that the MAC waves will only be affected by the differential rotation when $R_m \gtrsim O(1)$. So for $\Lambda = O(1)$ and $R_m = O(1)$ we expect $R_c = O(q^{-1})$ for MAC waves. Thus the diffusive thermal instability may no longer be the most easily excited when a strong shear is present.

There is clearly a need to investigate the effect of differential rotation on the other classes of hydromagnetic instability present in rapidly rotating systems. Our picture

of which classes are important in the various regions of the Λ , q parameter space has been built upon results for uniformly rotating systems. As we have seen, this may be quite misleading if applied to a differentially rotating system. Some progress has been made by Braginsky (1980), who investigated the effect of differential rotation on MAC waves. He found a shortening of lengthscale throughout the fluid but he was unable to incorporate diffusion (which must become important as the lengthscale decreases) at the same time as buoyancy. Work is in progress to remove the restriction $q = 0$ and extend the present study to MAC waves and other instabilities operating on or about the magnetic diffusion timescale.

At this stage it is possible only to speculate on the role that differential rotation plays in the application of the theory of hydromagnetic waves to the geomagnetic secular variation. Both diffusive (present work) and non-diffusive (Braginsky 1980) theories exhibit the tendency for the instability to be concentrated, although the mechanism and the details are different. If the toroidal field is much larger than the poloidal field then the magnetic Reynolds number based on the azimuthal flow must be large ($R_m \gg 1$). In such a case we expect that magnetic-field perturbations may be strongly localized. As a consequence, we would expect the magnetic field observed at the Earth's surface to be a consequence of waves generated close to the mantle-core boundary. The observed secular variation will be due to a combination of the fluid motion in that region and the phase speed of the wave relative to the fluid. Which is the more important will depend on the strength R_m of the flow and the nature of the instability generating the wave.

This work was funded by the Science and Engineering Research Council of Great Britain.

Appendix A

There are many established numerical methods for solving one-dimensional boundary-value problems, but often special care must be taken when a critical layer is present. For example a standard shooting method fails unless combined with some technique like orthonormalization (see Davey 1973, 1978). If a matrix method is used, however, the presence of a critical layer causes no trouble provided that a sufficient number of grid points is used to resolve the layer. There is little to choose between shooting with orthonormalization and a matrix method using inverse iteration (see I; Peters & Wilkinson 1971*a*) provided that fourth-order finite differences are used. Unpublished comparisons between these two methods applied to the Orr-Sommerfeld problem show that the time taken to achieve the same accuracy is similar, with the inverse-iteration matrix method perhaps about 10% faster in the cases looked at. We therefore adopt this latter method, since the extra storage necessary is not a critical factor in a one-dimensional problem.

The interval $0 \leq z \leq 1$ is divided into N sections and the system of equations (2.7) is transformed into a set of difference equations using fourth-order finite differences (whose error is $O(N^{-4})$). The resulting matrix eigenvalue problem is of the form

$$\mathbf{Ax} = p\mathbf{Bx}, \quad (\text{A } 1)$$

where \mathbf{B} is diagonal and \mathbf{A} is banded with bandwidth 25. This system was solved using inverse iteration coded in such a way that only the non-zero band of \mathbf{A} is stored and up to 700 grid points could be accommodated. The procedure adopted to obtain the

results given in §3 was to take as a starting point the $R_t = 0$ solution from S79 and gradually increase R_t . This worked well, but it has one drawback – for $R_t = 0$ we know we are looking at the most-unstable mode, but for $R_t > 0$ there is no guarantee. To check that the mode followed from $R_t = 0$ remains the most unstable it is necessary to find the growth rates of the other modes. The only sure way to do this is to use a matrix method which finds all the eigenvalues of the system. In adapting (A 1) for use with the *LR* algorithm (Peters & Wilkinson, 1971*b*), round-off errors became a problem so an alternative formulation was used. In place of finite differences, a Fourier expansion of the variables b , j , and θ in (2.7) was used and a matrix equation of the form

$$\mathbf{C}\mathfrak{g} = p\mathfrak{g} \quad (\text{A } 2)$$

constructed. The matrix \mathbf{C} is not banded, so the full matrix must be stored, but this is necessary anyway when finding all the eigenvalues. The results of this method are in agreement with those obtained by finite differences/inverse iteration and they confirm that the most unstable mode followed from $R_t = 0$ remains the most-unstable mode when $R_t > 0$.

Appendix B

We have seen from the numerical results that for the thermally driven instabilities the most-unstable mode has $k^2 \gg 1$ when $R_T \gg 1$. The results also suggest that $R_c \sim R_t$ when there is no turning point for $\Omega(z)$, while $R_c \sim R_t^{\frac{1}{2}}$ otherwise. If we consider the former case first, and assume that $T = mR_t \gg 1$, and that $R_c = TS/\Lambda m^2$, then the equations can be reduced to the form

$$D^2w = -S\tilde{\mathfrak{g}}, \quad (\text{B } 1a)$$

$$w = i(\Omega(z) - \Omega(z_L))\tilde{\mathfrak{g}} - T^{-1}D^2\tilde{\mathfrak{g}}, \quad (\text{B } 1b)$$

where $\tilde{\mathfrak{g}} = T\mathfrak{g}$ and $p = -iT\Omega(z_L)$. The small term in $D^2\mathfrak{g}$ must be retained since it enables the thermal boundary layer to be constructed. We note that R_c is proportional to R_t and inversely proportional to Λ and m (*cf.* figure 1*a*). As in §4 it is instructive to form integrals of (B1):

$$S = \frac{T\langle |Dw|^2 \rangle}{\langle |D\tilde{\mathfrak{g}}|^2 \rangle}, \quad \langle (\Omega - \Omega(z_L))|\tilde{\mathfrak{g}}|^2 \rangle = 0. \quad (\text{B } 2)$$

Thus $S > 0$ (so the buoyancy-catalysed instability obeys different (and much more complicated) asymptotics), and also $0 < z_L < 1$, confirming the existence of the critical layer. The latter is of thickness $T^{-\frac{1}{2}}$, and within it $\mathfrak{g} \sim T^{\frac{1}{2}}$, so that the integral of \mathfrak{g} through the layer is of order unity. The problem can be solved asymptotically by finding the solutions to (B 1) with $T = \infty$ that vanish at $z = 0, 1$ respectively. Then S and z_L can be found by applying the conditions that w is continuous at $z = z_L$ and that Dw has a discontinuity that can be evaluated by consideration of the forced Airy equation that (B 1*b*) reduces to in the critical layer (see e.g. equation (4.23) of Braginsky & Roberts 1975). However, a full numerical solution of (B 1) is in fact much simpler, and the numerical results show that it is not a simple local condition which determines the location of the critical layer. Shear inhibits convection so we expect the preferred location of the critical layer to be where the shear is smallest. (Indeed this is the case when the shear vanishes; when $\Omega'(z)$ has a zero at $z = z_T$ convection is most easily driven when the critical layer is located at $z = z_T$.) There are other competing effects though. These are negligible when the shear has a zero in the layer,

but turn out to be significant when there is no zero. To test the effect of varying the profile of $\Omega(z)$ on the location of the critical layer we chose a modified version of the flow (3.1),

$$\Omega(z) = 1 - \alpha z - \beta z^2, \quad (\text{B } 3)$$

and investigated how z_L depends on α and β . With $\alpha = 0$, changing β has no effect on z_L since the ratio of the shears at two different locations is independent of β . With $\beta = 0$ and $\alpha = 1$, the shear is uniform throughout the layer and we find that location of the critical layer in mid-layer ($z_L = 0.5$) is very strongly favoured. (The critical value of S is $O(1)$, but, to drive convection in a critical layer at a different location ($z_L \neq 0.5$), a value of $S > O(100)$ was found to be required.) As far as the local conditions are concerned, there is nothing to distinguish $z = 0.5$ from any other value of z . Thus the effect of the boundaries must be important in determining the preferred location of the critical layer, and the absence of other competing effects the preferred location is at $z = 0.5$. If there is a gradient in the shear the competing effect is that the critical layer prefers to be located where the shear is least. The balance between these two effects was investigated by taking $\beta = 1$ and increasing α from zero. The case $\alpha = 0$ is that investigated in §3 with the flow (3.1). There $z_L \approx 0.4$. As α is increased, the shear becomes more uniform and, as we would expect, z_L increases and approaches 0.5 as α becomes large. In summary it is clear that the preferred location of the critical layer cannot be determined by a local condition when the shear is everywhere non-zero. Instead, it is a competition between the influence of the boundaries (which prefer $z_L = 0.5$) and the constraint of the shear (which prefers $z_L = z_m: |\Omega'(z_m)| \leq |\Omega'(z)|, 0 < z < 1$) which determines the preferred location of the critical layer.

It is the integral condition (B 2b) which is the key to determining z_L . The contribution to the integral from the critical layer is negligible since $|\tilde{\vartheta}|^2$ is symmetric, and $\Omega - \Omega(z_L)$ is antisymmetric about $z = z_L$. The imaginary part $\tilde{\vartheta}_i$ of $\tilde{\vartheta}$ is small compared with the real part $\tilde{\vartheta}_r$ outside the critical layer ($\tilde{\vartheta}_r = O(Z^{-1})$ while $\tilde{\vartheta}_i = O(Z^{-4})$ as $Z \rightarrow \infty$, where $Z = T^{\frac{1}{2}}(z - z_c)$), so the dominant contribution to (B 2b) is $(\Omega - \Omega(z_L))|\tilde{\vartheta}_r|^2$ integrated over the mainstream. Since $\tilde{\vartheta}_i$ is small in the mainstream, (B 1a) can be approximated by $D^2w = 0$, and we can approximate the profile of w_i by

$$w_i = \frac{z}{z_c} \quad (z < z_c), \quad w_i = \frac{1-z}{1-z_c} \quad (z > z_c). \quad (\text{B } 4)$$

In the mainstream, (B 1b) gives $(\Omega - \Omega(z_m))\tilde{\vartheta}_r = w_i$, so the approximate condition determining the position of the critical layer is

$$\lim_{\epsilon \rightarrow 0} \left\{ \int_0^{z_L - \epsilon} \frac{z^2}{z_L^2(\Omega(z) - \Omega(z_L))} dz + \int_{z_L + \epsilon}^1 \frac{(1-z)^2}{(1-z_L)^2(\Omega(z) - \Omega(z_L))} dz \right\} = 0. \quad (\text{B } 5)$$

This condition was tested for $\Omega(z)$ given by (B 3), and the results were found to be in excellent agreement with those obtained by numerical solution of (B 1). Typically the difference between the two answers is less than 0.1%. In the case $\beta = 0$, (B 5) reduces to $\ln(z_L/(1-z_L)) = 0$, whose solution is $z_L = 0.5$, as was found numerically.

REFERENCES

- ACHESON, D. J. 1972 On the hydromagnetic stability of a rotating fluid annulus. *J. Fluid Mech.* **52**, 529–541.
- ACHESON, D. J. 1973 Hydromagnetic wavelike instabilities in a rapidly rotating stratified fluid. *J. Fluid Mech.* **61**, 609–624.
- ACHESON, D. J. 1978 Magneto-hydrodynamic waves and instabilities in rotating fluids. In *Rotating Fluids in Geophysics* (ed. P. H. Roberts & A. M. Soward), pp. 315–349. Academic.
- ACHESON, D. J. 1980 Stable density stratification as a catalyst for instability. *J. Fluid Mech.* **96**, 723–733.
- ACHESON, D. J. 1982 Thermally convective and magneto-hydrodynamic instabilities of a rotating fluid I. Unpublished manuscript.
- ACHESON, D. J. & HIDE, R. 1973 Hydromagnetics of rotating fluids. *Rep. Prog. Phys.* **36**, 159–221.
- BRAGINSKY, S. I. 1967 Magnetic waves in the Earth's core. *Geomag. Aeron.* **7**, 851–859.
- BRAGINSKY, S. I. 1980 Magnetic waves in the core of the Earth. II. *Geophys. Astrophys. Fluid Dyn.* **14**, 189–208.
- BRAGINSKY, S. I. & ROBERTS, P. H. 1975 Magnetic field generation by baroclinic waves. *Proc. R. Soc. Lond. A* **347**, 125–140.
- DAVEY, A. 1973 A simple numerical method for solving Orr–Sommerfeld problems. *Q. J. Mech. Appl. Maths* **26**, 401–411.
- DAVEY, A. 1978 Numerical methods for solution of linear differential eigenvalue problems. In *Rotating Fluids in Geophysics* (ed. P. H. Roberts & A. M. Soward), pp. 485–498. Academic.
- ELTAYEB, I. A. 1981 Propagation and stability of wave motions in rotating magnetic systems. *Phys. Earth Planet. Interiors* **24**, 259–271.
- FARN, D. R. 1979 Thermal and magnetic instabilities in a rapidly rotating fluid sphere. *Geophys. Astrophys. Fluid Dyn.* **14**, 103–126.
- FARN, D. R. & PROCTOR, M. R. E. 1983 [I] Hydromagnetic waves in a differentially rotating sphere. *J. Fluid Mech.* **128**, 1–20.
- PETERS, G. & WILKINSON, J. H. 1971*a* The calculation of specified eigenvectors by inverse iteration. In *Handbook for Automatic Computation*, vol. 2: *Linear Algebra* (ed. J. H. Wilkinson & C. Reinsch), pp. 418–439. Springer.
- PETERS, G. & WILKINSON, J. H. 1971*b* Eigenvalues of real and complex matrices by *LR* and *QR* triangularisations. In *Handbook for Automatic Computation*, vol. 2: *Linear Algebra* (ed. J. H. Wilkinson & C. Reinsch), pp. 370–395. Springer.
- ROBERTS, P. H. 1978 Magneto-convection in a rapidly rotating fluid. In *Rotating Fluids in Geophysics* (ed. P. H. Roberts & A. M. Soward), pp. 421–435. Academic.
- ROBERTS, P. H. & LOPER, D. E. 1979 On the diffusive instability of some simple steady magneto-hydrodynamic flows. *J. Fluid Mech.* **90**, 641–668.
- ROBERTS, P. H. & SOWARD, A. M. 1972 Magneto-hydrodynamics of the Earth's core. *Ann. Rev. Fluid Mech.* **4**, 117–154.
- SOWARD, A. M. 1979 [S79] Thermal and magnetically driven convection in a rapidly rotating fluid layer. *J. Fluid Mech.* **90**, 669–684.